Scientific Papers. Series E. Land Reclamation, Earth Observation & Surveying, Environmental Engineering. Vol. XV, 2026
Print ISSN 2285-6064, CD-ROM ISSN 2285-6072, Online ISSN 2393-5138, ISSN-L 2285-6064

INFLUENCE OF CONSTITUTIVE MODELS ON DEEP EXCAVATIONS: A COMPARATIVE STUDY

Daniel-Marcel MANOLI, Nicolae RĂDULESCU-SINGURAN, Adrian Alexandru SAVU, Elena-Mihaela STAN, Cristian-Ștefan BARBU

Technical University of Civil Engineering of Bucharest, 122-124 Lacul Tei Blvd, District 2, Bucharest, Romania

Corresponding author email: daniel.manoli@utcb.ro

Abstract

Accurate prediction of soil–structure interaction is essential for the safe design of deep excavations in urban environments. This paper presents a three-dimensional numerical investigation assessing the influence of different soil constitutive models on the predicted behavior of a deep excavation. Finite element analyses were carried out using the Mohr–Coulomb (MC), Hardening Soil (HS), and Hardening Soil with Small-Strain Stiffness (HSS) models, applied to a real excavation case supported by retaining walls. The comparative study focuses on excavation-induced stress redistribution and horizontal wall deformations. The results indicate that the MC and HS models overestimate wall deformations, whereas the HSS model offers a significantly improved prediction due to its ability to capture soil stiffness at small strain levels. The study confirms that incorporating small-strain stiffness is critical for realistic deformation assessment and reliable design of deep excavations.

Key words*: constitutive model, deep excavation, MEF.*

INTRODUCTION

Due to the continuous development of urban areas, it is necessary to choose modern solutions for carrying out new buildings. At present, vertical development of civil buildings is preferred, including a significant number of underground levels that require deep excavations in the vicinity of existing structures, without affecting their functionality. Thus, to analyse the behaviour of the retaining structure, the finite element method (FEM) is often used. In order to obtain the best results, consistent with reality, it is necessary to have a good understanding of the calculation method, the constitutive models used to model different soil types or structural elements, the mesh distribution, the calculation phases, and to consider the effects of the assumptions made.

The choice of constitutive model has a decisive influence on the predicted response of deep excavations, and this has been the subject of numerous comparative studies. Although the linear elastic–perfectly plastic Mohr-Coulomb model remains widely used in practice for its simplicity, it is generally recognised as inadequate for serviceability predictions, since it cannot reproduce the stress-dependent stiffness of soils or their markedly higher stiffness at small strains (Obrzud, 2010). The Hardening Soil model (Schanz et al., 1999) introduced a stress-dependent stiffness and a clear distinction between primary loading and unloading/reloading, while its extension to small strains (Benz, 2007) additionally captures the non-linear decay of stiffness from the very small-strain shear modulus. Comparative analyses of braced and anchored excavations have repeatedly shown that the Mohr-Coulomb model tends to overestimate wall deflections and to predict an unrealistic ground heave behind the wall, whereas the Hardening Soil model and, in particular, the Hardening Soil with small-strain stiffness model reproduce field-measured wall displacements far more closely (Lim et al., 2010; Teo & Wong, 2012; Dahal et al., 2024). Similar conclusions were reached by Herold & von Wolffersdorff (2009), who back-calculated two instrumented large-scale geosynthetic-reinforced earth structures and found that the HSsmall model almost exactly matched the measured horizontal displacements, while the Mohr-Coulomb model deviated clearly, over-predicting displacements at low surcharge and under-predicting them at high surcharge. The HSsmall model has likewise been applied

successfully to the probabilistic assessment of diaphragm walls (Kawa et al., 2021). These findings motivate the present comparative study, in which the three constitutive models are applied to the same real deep excavation supported by a diaphragm wall.

The Mohr-Coulomb (MC) constitutive model is a linear elastic perfectly - plastic model often used due to the small number of the required parameters and the ease with which they can be determined.

In the elastic domain, the model shows linear behavior based on Hooke's Law, defined by two parameters: Young's modulus (E), and Poisson's ratio (ν). In the plastic domain, the failure criterion is defined by two parameters: the internal friction angle (ϕ), and cohesion (c), also known as the shear resistance parameters. Additionally, the dilatancy angle (ψ) is used to describe the plastic volumetric strain variation.

According to the Mohr-Coulomb constitutive model, the soil will reach failure in shear, along an arbitrary plane when, due to the applied loads, the tangential stress is in a linear relationship with the normal stress, which is unique for each type of soil. Also, it is based on the use of the stress state at a point (Figure 1), that is, from a graphical point of view, the use of the Mohr circle. This circle represents all possible stress states (σ, τ) at a point when any plane with any orientation passing through that point is considered (Șerbulea, 2013).

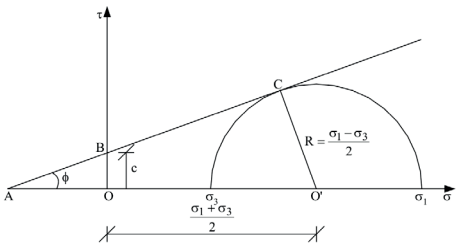


Figure 1. Stress state tangent to the intrinsic line (Șerbulea, 2013)

The equation that describes the Mohr-Coulomb failure criterion is given by:

$$\tau = \sigma \tan(\phi) + c$$

where τ is the tangential stress and σ is the normal stress.

If the pore water pressure is known, the effective shear strength parameters can be calculated:

$$\tau = \sigma' \tan(\phi') + c'$$

In the three-dimensional space of principal stresses, $\sigma_1 - \sigma_2 - \sigma_3$, the Mohr-Coulomb failure criterion is represented as a pyramid with a hexagonal base (Figure 2), whose axis lies along the trisectors $\sigma_1 = \sigma_2 = \sigma_3$.

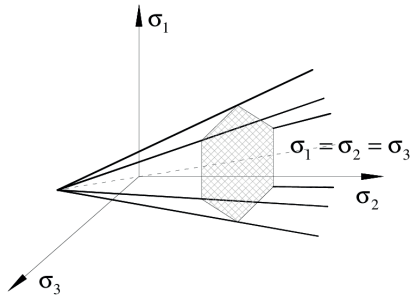


Figure 2. Mohr-Coulomb representation in the space of principal stresses (Popa & Batali, 2010)

In the space of principal stresses, a stress state will not result in failure as long as it remains inside the surface (Șerbulea, 2013).

The Hardening Soil (HS) model is an advanced constitutive model for representing the nonlinear-elastic-plastic behavior of soils, suitable for both soft and stiff soil types (Schanz et al., 1999).

When subjected to a deviatoric stress, soil exhibits a decrease in stiffness and simultaneously undergoes plastic deformations. The relationship between deviatoric stress and axial strain is most readily observed in a triaxial compression test and can be approximated by a hyperbolic curve (Figure 3) (Brinkgreve et al., 2023).

The principal characteristics of the nonlinear Hardening Soil constitutive model are:

- Stiffness depends on the stress, as defined by the parameter m;
- Plastic straining due to primary deviatoric loading, represented by the parameter E_{50}^{ref} (secant stiffness in a standard drained triaxial test);
- Plastic straining due to primary compression, represented by the parameter E_{oed}^{ref} (tangent stiffness for primary oedometer loading);
- Elastic unloading/reloading, represented by the parameters E_{ur}^{ref} (unloading/reloading stiffness) and ν_{ur} (Poisson's ratio for unloading/reloading);
- The failure criterion used is Mohr-Coulomb,

characterized by the parameters ϕ, c, and ψ (Brinkgreve et al., 2023).

A basic concept of the model is the hyperbolic relationship between the vertical strain, ε_1, and the deviatoric stress, q.

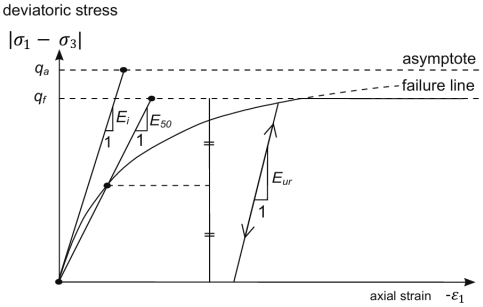


Figure 3. The hyperbolic stress-strain relationship resulting from the drained triaxial test (Brinkgreve et al., 2023)

The advantage of the Hardening Soil model lies not only in the use of a hyperbolic stress-strain curve instead of a bilinear curve, as in the Mohr-Coulomb model, but also in the stress-dependent stiffness of the soil. In the Mohr-Coulomb model, a fixed value of the Young's modulus is used, whereas in reality this value depends on the magnitude of the stress (Brinkgreve et al., 2023).

The Hardening Soil constitutive model assumes elastic behavior during unloading and reloading. However, the strain range within which soil can be considered elastic is very small. With increasing strain, the shear stiffness of the soil decreases in a nonlinear manner.

Figure 4 shows the variation of the soil stiffness with shear strain.

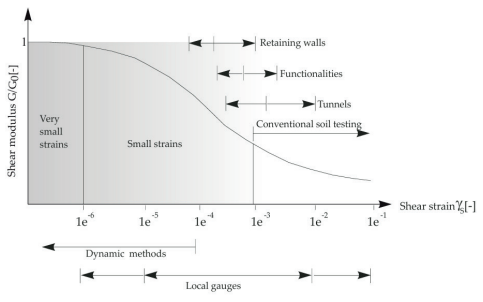


Figure 4. Hardening Soil with small strain model stiffness - strain behavior of soil (Brinkgreve et al., 2023)

The characteristics shear strains that can be measured near geotechnical structures, as well as the strain range applicable in laboratory tests, are also represented. It can be observed that, for the minimum strains that can be measured in laboratory tests, the soil stiffness decreases to about half of its initial value (Brinkgreve et al., 2023).

Compared to the Hardening Soil model, the Hardening Soil with small strain (HSSS) model assumes the use of additional parameters (Benz, 2007):

- The reference shear modulus at very small strains ($\varepsilon < 10^{-6}$), G_0^{ref};
- The shear strain corresponding to 70% of the value of G_0^{ref}, $\gamma_{0.7}$.

MATERIALS AND METHODS

For this study, in order to compare the three constitutive models descried above, the 3D finite element method was used. Thus, the same case study was modelled using the Mohr-Coulomb, Hardening Soil and the Hardening Soil with small strain models. The numerical modelling was carried out using Plaxis 3D software.

The case study project is located in the city of Timișoara, Romania. It is a building with two basements and three stories above the ground. Therefore, an excavation depth of 6.80 m is required to construct the two basements' levels. The retaining structure solution consists of a diaphragm wall with a thickness of 0.45 m and a depth of 11.00 m (Figure 5). At the top of the diaphragm wall, a capping beam with a height of 0.45 m and a width of 0.60 m is provided.

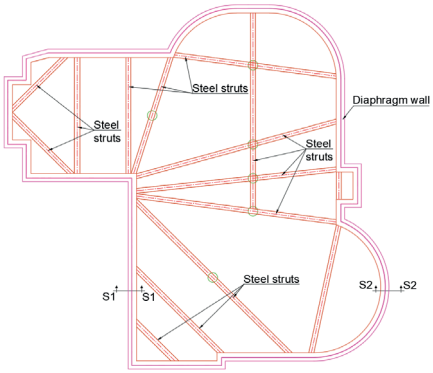


Figure 5. Layout of the excavation site

To limit the lateral displacements of the diaphragm wall, one level of bracing struts was used. The bracing strut system consists of circular steel hollow sections with a diameter of 610 mm and a thickness of 10 mm, spaced at approximately 6 m intervals, installed at a depth of 2.00 m.

In the three - dimensional finite element software, the diaphragm wall was modelled as plate elements, the capping beam as beam elements, and the steel struts as node-to-node anchors. The linear elastic constitutive model was used for both diaphragm wall and capping beam. Thus, the concrete modulus of elasticity is $3.1 \cdot 10^7$kPa, the Poisson's ratio is 0.2 and the unit weight is 25kN/m^3.

The site investigations consist of four geotechnical boreholes with a maximum depth of 22.00m and four light dynamic penetration tests (DPM) with a maximum depth of 15.00m. Based on these in situ investigations and the results of the laboratory tests, the soil stratigraphy and parameters are presented in Figure 6, Table 1 and Table 2.

Table 1. Soil stratigraphy

Soil layer	Depth [m]	Soil layer description
1	0.00÷ -0.70/2.10	Fill composed of construction debris mixed with clay, sand and gravel
2	-0.70/-2.10÷ -2.30/2.70	Clay to sandy silty clay, grey, with reddish intercalation, stiff.
3	-2.30/2.70÷ -7.00/10.10	Fine sand to silty sand, grey, loose to medium dense toward the base of the layer.
4	-7.00/10.10÷ -11.10/12.30	Clay to silty clay, greyish-green, with yellowish intercalations, stiff.
5	-11.10/12.30÷ -22.00	Sand to silty sand, grey, dense.

Table 2. Soil parameters used in the numerical analysis

Soil type	Γ	γ_{sat}	E_{50}^{ref}	E_{oed}^{ref}	E_{ur}^{ref}	ν_{ur}	c'	ϕ'	G_0	$\gamma_{0.7}$	R_{inter}
	[kN/m^3]	[kN/m^3]	[kPa]	[kPa]	[kPa]	[-]	[kPa]	[°]	[kPa]	[-]	[-]
1	18.50	19.50	7000	7000	21000	0.3	5	15	35669	0.00009	0.8
2	19.00	20.00	7500	7500	22500	0.3	32	17.2	68200	0.00026	0.8
3	19.00	20.00	8800	8800	26400	0.3	5	27	65572	0.00023	0.8
4	19.40	20.40	12000	12000	36000	0.3	38	18	133098	0.00024	0.8
5	19.60	20.60	17634	17634	52902	0.3	5	30	102265	0.00035	0.8

γ - Unit weight; γ_{sat} - Saturated unit weight; E_{50}^{ref} - Secant stiffness in standard drained triaxial test; E_{oed}^{ref} - Tangent stiffness for primary oedometer loading; E_{ur}^{ref} - Unloading/reloading stiffness; ν_{ur} - Poisson's ratio for unloading-reloading; c' - Effective cohesion; ϕ' - Effective angle of internal friction; G_0 - Shear modulus at very small strains; $\gamma_{0.7}$ - Shear strain corresponding to 70% of the value of G_0; R_{inter} - Strength reduction factor.

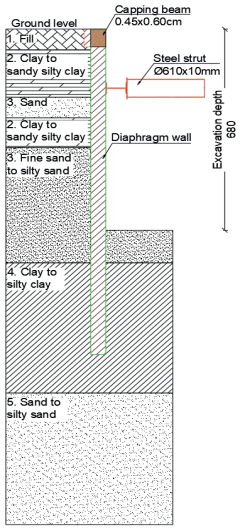


Figure 6. Construction phases and soil stratigraphy

The soil parameters required for the HSSS model were determined based on field investigations.

The finite element calculation phases, which correspond to the in-situ execution stages, are:

- Generation of the initial stress state;
- Installation of the diaphragm wall and the capping beam;
- Lowering of the groundwater level;
- Excavate to 3.00 m below the ground level;
- Installation of the bracing strut level;
- Excavation to the final depth of 6.80 m;
- Execution of the raft foundation and the slab over the second basement.

In order to perform finite element calculations, the numerical model was discretized into finite elements using a fine mesh.

RESULTS AND DISCUSSIONS

The lateral displacements of the retaining structure

Figure 7 shows the lateral displacement diagrams of the diaphragm wall for Section 1 (S1-S1), for the three constitutive models considered: Mohr-Coulomb, Hardening Soil and Hardening Soil with Small Strain. Figure 8 shows the lateral displacement diagrams for Section 2 (S2-S2), which is located in the circular area of the diaphragm wall. The two sections were selected based on the maximum stress values, lateral displacements, and the in-plan configuration of the diaphragm wall.

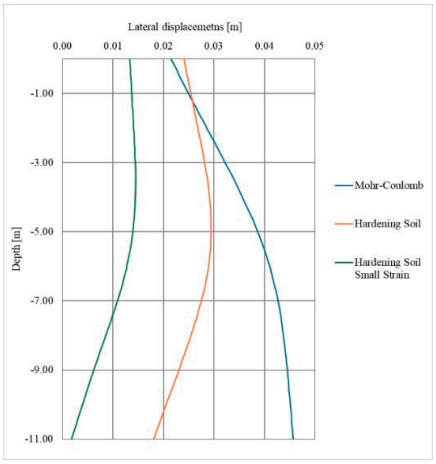


Figure 7. Lateral displacements of the retaining structure, Section 1

For both sections, the lateral displacement diagrams show that the Mohr-Coulomb constitutive model leads to the maximum lateral displacements of the retaining structure, while the minimum values are obtained when using the Hardening Soil with Small Strain constitutive model. In the case of the Mohr-Coulomb constitutive model, the maximum lateral displacement occurs in the lower part of the retaining structure, whereas for the other two constitutive models, it occurs in the upper part of the diaphragm wall. When comparing the Hardening Soil and Hardening Soil with Small Strain models, the latter results in a maximum lateral displacement that is approximately half of that obtained using the former model.

The differences between the two analysed sections are due to the in-plan shape of the retaining structure. Thus, for Section 2 (S2-S2), the lateral displacements are smaller than those in Section 1 (S1-S1), due to the circular shape of the diaphragm in this area and the resulting arching effect.

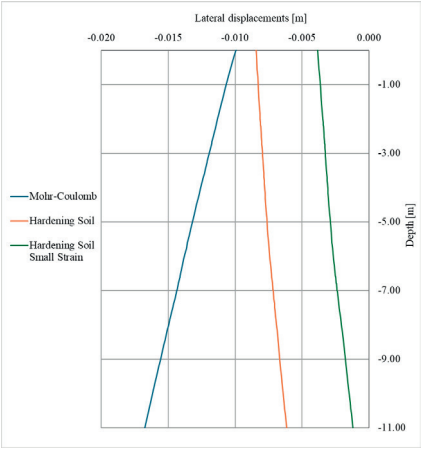


Figure 8. Lateral displacements of the retaining structure, Section 2

The bending moment of the retaining structure

Figure 9 and Figure10 shows the bending moment diagrams of the retaining structure for the three analysed constitutive models and the two section, S1-S1 and S2-S2.

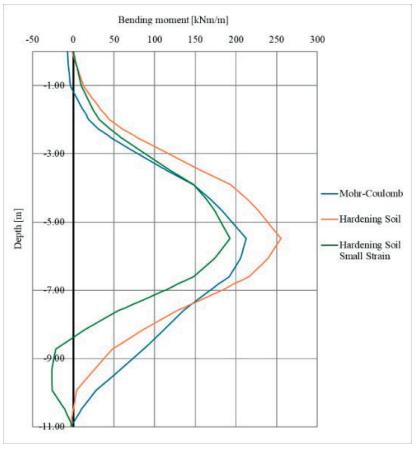


Figure 9. Bending moment diagrams - Section 1

In the case of Section 1 (S1-S1), where the diaphragm wall has a linear in-plan shape, the maximum bending moment occurs for the Hardening Soil constitutive model, while the

minimum value is obtained when the Hardening Soil with Small Strain model is used. For all constitutive models, the bending moment diagrams have a similar shape, and the maximum values occur at approximately the same depth, close to the final excavation depth.

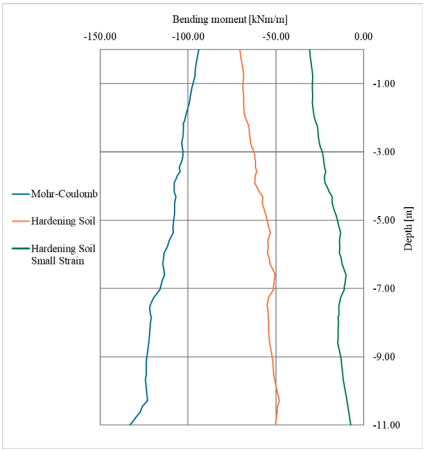


Figure 10. Bending moment diagrams - Section 2

In the case of Section 2 (S2-S2), where the diaphragm wall has a circular in-plan shape, the maximum bending moment occurs for the Mohr-Coulomb constitutive model, while the minimum value is obtained for the Hardening Soil with Small Strain model, similar to Section 1. Unlike Section 1, the maximum bending moment in Section 2 occurs in the upper part of the diaphragm wall for both the Hardening Soil and Hardening Soil with Small Strain models, and in the lower part of the retaining structure when the Mohr-Coulomb model is used.

In general, regardless of the constitutive model used, the maximum bending moments are smaller for Section 2 than for Section 1 due to the arching effect.

CONCLUSIONS

This paper presents a comparative study on the influence of the constitutive models used to simulate soil behavior. Three-dimensional finite element numerical models were developed for the same project using the Mohr-Coulomb, Hardening Soil and Hardening Soil with Small Strain constitutive models.

While the soil parameters required for the Mohr-Coulomb constitutive model can generally be determined from conventional geotechnical investigations and standard laboratory tests, the Hardening Soil model, and especially the Hardening Soil with small strain model, require more advanced in-situ and laboratory testing. The findings of this study demonstrate that the enhanced complexity of the Hardening Soil with small strain model leads to a more realistic representation of the retaining structure behavior compared to simpler constitutive models, regardless of the structure's in-plan configuration.

REFERENCES

Benz, T. (2007). *Small-Strain Stiffness of Soils and its Numerical Consequences*. PhD thesis, University of Stuttgart, Germany.

Brinkgreve, R. B. J., Kumarswamy, S., Swolfs, W. M., Fonseca, F., Zalamea, N., Manoj, N. R., Singh, K., Zampich, L., (2023). *Material Models Manual, Plaxis 3D.* U.S.: Bentley Systems Incorporated

Herold, A., & von Wolffersdorff, P.-A. (2009). The use of Hardening Soil Model with Small-Strain Stiffness for Serviceability Limit State analyses of GRE structures. *Proceedings of GeoAfrica 2009*, Cape Town, South Africa.

Kawa, M., Puła, W., & Truty, A. (2021). Probabilistic analysis of the diaphragm wall using the hardening soil-small (HSs) model. *Engineering Structures*, 232, 111869.

Dahal, B. K., Regmi, S., Paudyal, K., Dahal, D., & Kc, D. (2024). Enhancing deep excavation optimization: Selection of an appropriate constitutive model. *CivilEng*, 5(3), 785–800.

Lim, A., Ou, C. Y., & Hsieh, P. G. (2010). Evaluation of clay constitutive models for analysis of deep excavation under undrained conditions. *Journal of GeoEngineering*, 5(1), 9–20.

Obrzud, R. F. (2010). On the use of the Hardening Soil Small Strain model in geotechnical practice. *Numerics in Geotechnics and Structures (ZSoil Day)*, Lausanne, Switzerland.

Popa, H., & Batali, L. (2010). Using Finite Element Method in geotechnical design. Soil constitutive laws and calibration of the parameters. Retaining wall case study. *WSEAS Transactions on applied and theoretical mechanics*, 5(3), 177-186.

Schanz, T., Vermeer, P. A., & Bonnier, P. G. (1999). The Hardening Soil model: Formulation and verification. In R. B. J. Brinkgreve (Ed.), *Beyond 2000 in Computational Geotechnics*, 281–296. Rotterdam: Balkema.

Şerbulea, M. S. (2013). *Mecanica avansată a pământurilor*. Bucharest, RO: Printech.

Teo, P. L., & Wong, K. S. (2012). Application of the Hardening Soil model in deep excavation analysis. *The IES Journal Part A: Civil & Structural Engineering*, 5(3), 152–165.